Soft Matter

Accepted Manuscript

This article can be cited before page numbers have been issued, to do this please use: N. Wilke, J. Bugase, L. Treffenstädt and T. M. Fischer, *Soft Matter*, 2017, DOI: 10.1039/C7SM01475A.

ROYAL SOCIETY OF CHEMISTRY

rsc.li/soft-matter-journal

View Article Online
DOI: 10.1039/C7SM01475A

Journal Name

ARTICLE TYPE

Cite this: DOI: 10.1039/xxxxxxxxxx

Wrinkled labyrinths in critical demixing ferrofluid.

Natalia Wilke[a,b], Jonas Bugase[b], Lisa-Marie Treffenstädt[b] and Thomas M. Fischer[b]

Received Date
Accepted Date

DOI: 10.1039/xxxxxxxxxx

www.rsc.org/journalname

A thin film of a critical ferrofluid mixture undergoes a sequence of transitions in a magnetic field. First the application of a field induces a critical demixing of the fluid into cylindrical droplets of the minority phase immersed in an extended majority phase. At a second critical field the cylindrical shape is destabilized and transforms into a labyrinth pattern. A third wrinkling transition occurs at even higher field if the liquid has a liquid/air interface. The wrinkling is absent if the droplet has a cover-slide on top. We explain the wrinkling by the wetting behavior of the liquid/air interface that shifts the surface region away from a critical demixing point.

Wrinkles are a result of two coupled materials that grow with different rates. The faster growing material must wrinkle since this is the only way to remain coupled with the other material. When we couple two solids with Hookian mechanical properties and the growth stops, elastic stresses in both materials hold the wrinkle in place[1]. The elastic theory of wrinkling has found useful applications in thin layers of graphene[2], thin polymer films[3], as well as in human skin[4].

Fluids in contrast to solids cannot support shear stress and one therefore needs long range interactions active on the geometric scale of the wrinkles to support their shape. Fluids with long range dipolar interactions can form modulated phases[5] that under proper conditions and in very different materials such as ferrofluids[6–14], dielectric liquids[15,16], Langmuir monolayers[17–20] or magnetic garnet films[21,22] can form undulated labyrinth patterns. Like wrinkles in solids they can occur either on a single[1] or on a hierarchy of length scales[23]. Here we show the formation of wrinkles of two length scales in a critical[24,25] ferrofluid mixture[26–31] that decomposes into two phases under the application of an external magnetic field. While the transition to a labyrinth pattern at a larger length scales is well known from immiscible ferrofluid mixtures[6–13] a second wrinkling transition at a higher wrinkling transition field is a new phenomenon occurring only in critical demixing ferrofluids.

We performed experiments with a ternary mixture of liquids (ester based ferrofluid/2,6-lutidine/silicone, see[32] for further details) and placed an approximately 40 micron thick droplet of $4\mu L$ on top of a silicon wafer exposing its free surface toward the air on top. Figure 1 shows reflection microscopy images of the texture of the liquid/air surface at different applied magnetic field (see also the video clip in[35]). At vanishing field (figure 1 a) the liquid mixture exhibits a single one phase homogeneous region of low reflectivity that shows no texture. At a critical field $H_{dem} \cong 0.7\,\mathrm{mT}$ the liquid demixes into a darker minority phase and a brighter majority phase (figure 1 b). The minority phase appears as a collection of drops with circular cross section. In a previous paper[32] we have shown that the three dimensional shape of the droplet is a cylinder that extends from the bottom of the film to the top. These cylinders are immersed in the majority phase. When we surmount a second critical field $H_{lab} = 2.6\,\mathrm{mT}$ (figure 1c) the circular cross section of the minority droplet deforms in to a dogbone shape[36] that for larger fields deforms into a labyrinth pattern of droplets (figure 1 d-g), with each of the droplets following intertwined two dimensional winding paths with a typical radius of curvature of the order of $100\,\mu\mathrm{m}$. This path significantly grows as a function of the external field as the two ends of the droplet explore regions that are not yet occupied by the minority phase. The increase of the external field is done with an adiabatically slow rate of $dH/dt = 0.04$ mT/s to prevent branching[14,18–20] of the droplets. This transition from circles to dog-bones and then to labyrinths have been largely described in ferromagnetic fluids[6–14] as well as in other systems[15–22]. At a third field $H_{wr} \cong 4.5\,\mathrm{mT}$ the path not only grows at the ends but ex-

[a] CIQUIBIC-CONICET,Facultad de Ciencias Químicas, Universidad Nacional de Córdoba, Argentina
[b] Institute of Physics, Universität Bayreuth, 95440 Bayreuth, Germany.

View Article Online
DOI: 10.1039/C7SM01475A

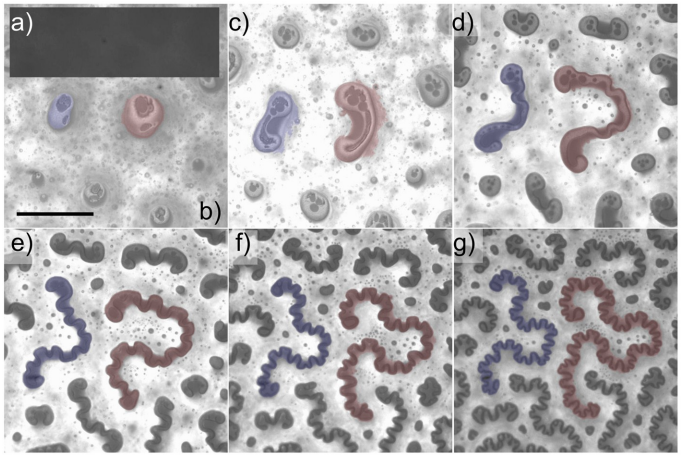

Fig. 1 Reflection microscopy image of the surface of a ferrofluid/2,6-lutidine/silicone (3:1:1) mixture at an external magnetic induction of a) $\mu_0 H = 0\,\mathrm{mT}$, b) $\mu_0 H = 2.4\,\mathrm{mT}$ c) $\mu_0 H = 3.6\,\mathrm{mT}$, d) $\mu_0 H = 4.8\,\mathrm{mT}$, e) $\mu_0 H = 6.3\,\mathrm{mT}$, f) $\mu_0 H = 7.9\,\mathrm{mT}$, g) $\mu_0 H = 9.3\,\mathrm{mT}$ normal to the film having a silicone oxide support and a free liquid/air surface at the top. a) exhibits a homogeneous image with no texture. The demixing of the fluid into ferrofluid rich and ferrofluid poorer phases occurs between a) and b). Cylindrical droplets get deformed into a labyrinth of droplets as one increases the field. The onset of the large scale shape transition is between b) and c). Between c) and d) the labyrinth starts to wrinkle. Wrinkles and large scale bending of the droplets can be distinguished very clearly as the droplets grow d)-g). Scale bar in figure b) is 100 μm. The two droplets in the center that are marked in blue and red corresponds to the data shown in Fig. 5. A video clip of the sequence of transitions can be viewed in [35].

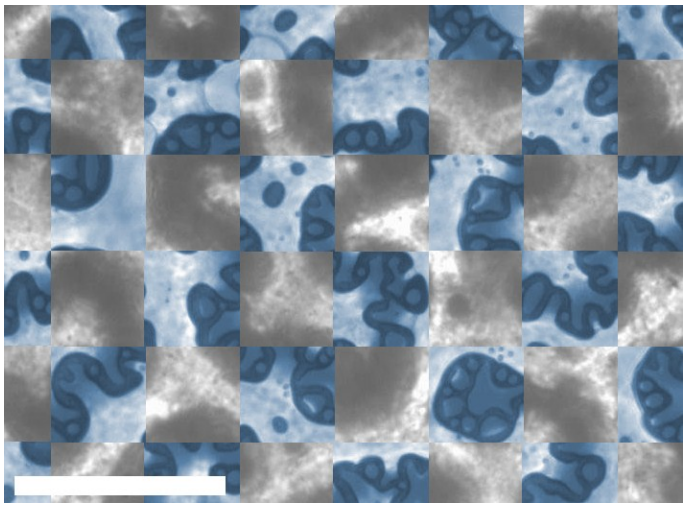

Fig. 2 Reflection microscopy image of a ferrofluid/2,6-lutidine/silicone (3:1:1) mixture at an external magnetic induction of $\mu_0 H = 9.3\,\mathrm{mT}$. We show checker-board sections of the surface (blue squares) and the bulk (gray squares). Small scale wrinkling can only be observed at the air/liquid interface. The scale bar is 100 μm.

hibits wrinkles of lower radius of curvature of the order of $20\,\mu$m. These wrinkles can be clearly distinguished from the large scale undulation of the droplet in the labyrinth pattern. This wrinkling transition has not been previously reported, and seems particular to critical demixing ferrofluids.

Figure 2 shows a checkerboard of two microscope images of the same region, one type of squares focused at the air/liquid interface the other squares focused in the bulk. The wrinkles can be observed only at the surface of the liquid. If we move the focal plane of the microscope into the bulk [33] the wrinkles disappear, while the large scale undulations persist.

The nature of the top surface has a strong effect on the observed pattern. Figure 3 shows reflection microscopy images of the same liquid as the one in figure 1, but the liquid is covered by a glass slip that replaces the liquid/air interface with a liquid/glass interface. The texture of the liquid under these circumstances is the same, however, without the small scale wrinkles. We can observe a demixing transition and a shape transition but no wrinkling. The wrinkling transition is also absent (data not shown) when using hydrophobic unbreakable plastic coverslips, or silanized cover slips as the top surface.

In order to quantify the wrinkles we introduce two metrics (see figure 4), one measuring the path length $s - s'$ of a segment of the droplet path, and a second by measuring the short cut length $|\mathbf{r}(s) - \mathbf{r}(s')|$ between the segment ends. By collecting all possible segments of length $s - s'$ of the droplet we may average the shortcut length over these segments. The logarithm of the ratio of the segment versus average short cut length defines our wrinkle number:

$$wr(s - s') = \ln \frac{s - s'}{< |\mathbf{r}(s) - \mathbf{r}(s')| >} \qquad (1)$$

The larger wr the more travel distance we save by taking the short cut instead of the segment path. In figure 4 we plot the wrinkle number as a function of the segment length for a fixed value of H for the red droplet in fig. 1g (black data points) and for the central droplet in fig. 3f. (gray data points) [34]. For both droplets the wrinkle number increases with the segment length starting at the noise level of the digitization of the image. The small scale wrinkles of the droplet of fig. 1g can be clearly seen in the black data as a region of negative curvature in this plot. The increase in the wrinkle number takes a rest when we have surmounted the typical path length ($\approx 30\,\mu$m) of a small scale wrinkle. It is therefore possible to introduce an intermediate path lengths b that short cuts the small scale wrinkles but not the long scale undulations (blue line in figure 4). This allows to subdivide the wrinkle number of the full length droplet into a short scale wrinkle number $wr_<$ and a large scale wrinkle number $wr_>$ for each value of the magnetic field, where the short scale wrinkling is the logarithm of the ratio of the total path length S of the droplet at the surface versus the total intermediate path length B of the bulk of the

View Article Online
DOI: 10.1039/C7SM01475A

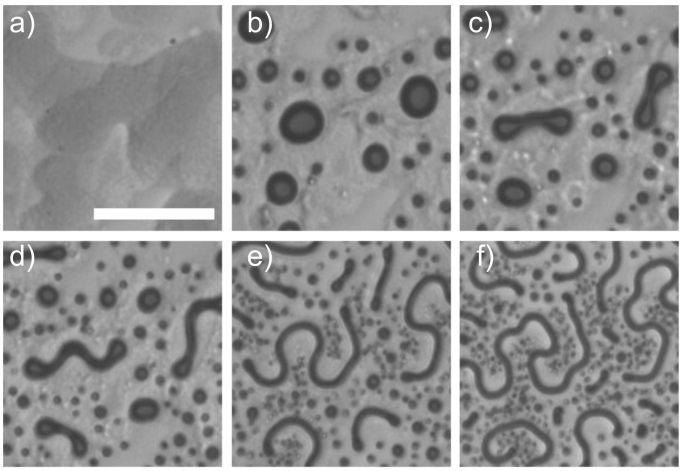

Fig. 3 Reflection microscopy image of a ferrofluid/2,6-lutidine/silicone (3:1:1) mixture at an external magnetic induction of a) $\mu_0 H = 0.1\,\mathrm{mT}$, b) $\mu_0 H = 2.9\,\mathrm{mT}$ c) $\mu_0 H = 3.6\,\mathrm{mT}$, d) $\mu_0 H = 4.8\,\mathrm{mT}$, e) $\mu_0 H = 6.3\,\mathrm{mT}$, f) $\mu_0 H = 9.3\,\mathrm{mT}$, normal to the film having a silicone oxide support and a glass cover slip surface at the top. a) exhibits a homogeneous image with no texture. Demixing of the fluid into ferrofluid enriched and ferrofluid poorer phases occurs between a) and b). The cylindrical droplets get deformed into a labyrinth droplet as one increases the field. The onset of the shape transition is between b) and c). Between c) and d) start to elongate. No wrinkling is observed at higher fields. Scale bar in figure a) is 100 μm.

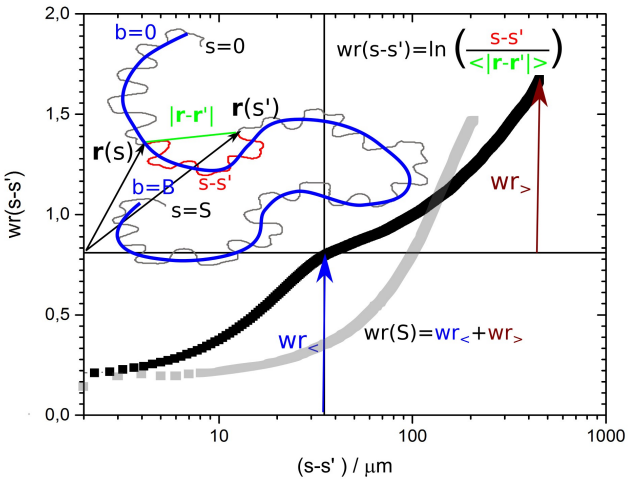

Fig. 4 Plot of the wrinkle number versus the segment length at a magnetic field of $9.3\,\mathrm{mT}$ (black c.f. fig 1g) for the free surface and (gray c.f. fig. 3f) for the glass covered surface. The free surface data exhibits a knee such that the total wrinkle number can be divided into the sum of the small scale wrinkle number $wr_<$ and the large scale wrinkle number $wr_>$ by introducing the intermediate bulk path length (blue line). No such knee is observed in the data from the glass covered surface of fig 3f.

droplet:

$$wr_< = \ln(S/B) \tag{2}$$

and

$$wr_> = \ln(B/|\mathbf{r}(S) - \mathbf{r}(0)|). \tag{3}$$

No such separation of length scale is observed in the gray data of the non-wrinkled labyrinth droplet of figure 3f.

In figure 5 we plot both wrinkle numbers, $wr_<$ and $wr_>$, of the red droplet of fig. 1 versus the external magnetic induction. It can be clearly seen that the onset of the small scale wrinkling is at a different field than the critical field H_{lab} for the shape transition toward the labyrinth, measured by either the onset of the large scale wrinkle number $wr_>$ or the surface path length S. The shape transition from circular toward dogbone and labyrinth patterns of non critical mixtures has been well studied and one can write the path length S or B of a droplet as

$$S, B = A_{s,b}/\xi_{s,b}\, \exp\left(-\frac{1}{2N_{Bo}^{s,b}}\right) \tag{4}$$

where $N_{Bo}^{s,b} = (\Delta\chi^{eff})^2 t_{s,b}\mu_0 H^2/2\sigma_{s,b}$ is the magnetic bond number with $t_{s,b}$ the thickness in the direction normal to the silicon oxide surface and $A_{s,b}$ the lateral area of the droplet, $\xi_{s,b}$ and $\sigma_{s,b}$, the width and the interfacial tension of the interface between the two phases, and $\Delta\chi^{eff}$ the effective susceptibility contrast between the two phases[37]. The index s corresponds to the droplet properties at the surface, while the index b indicates the same properties in the bulk of the liquid. The shape transition is a result of the competition of repulsive dipolar interactions within the droplet trying to elongate the droplet and the interfacial tension between the two phases trying to render the droplet shape circular.

Here we study a system that is close to a critical demixing point. It is clear that the wetting behavior of the liquid with any surface will alter the demixing behavior, either by moving the interfacial liquid closer or further from the critical demixing point. If the surface happens to move the interfacial liquid further from the critical demixing point, then the contrast between the two liquids will increase ($\sigma_s/t_s > \sigma_b/t_b$ or $N_{Bo}^s < N_{Bo}^b$) and the domain wall width between the two phases will decrease close to the surface ($\xi_s < \xi_b$).

The total free energy can be divided into a surface and a bulk part, and both are (almost) extensive in the thicknesses $t_s < t_b$ of each region. It is therefore reasonable to assume the surface to be enslaved by the bulk. The bulk droplet will therefore assume its equilibrium path length independent of the surface. When the bulk droplet shape becomes unstable the length of the droplets grows relatively slow with the magnetic field compared to the surface because of its smaller Bond number.

The area of the surface is smaller than that of the bulk at the onset of the shape instability. Therefore the initial length of the surface path is shorter than that of the bulk. However, the sur-

View Article Online
DOI: 10.1039/C7SM01475A

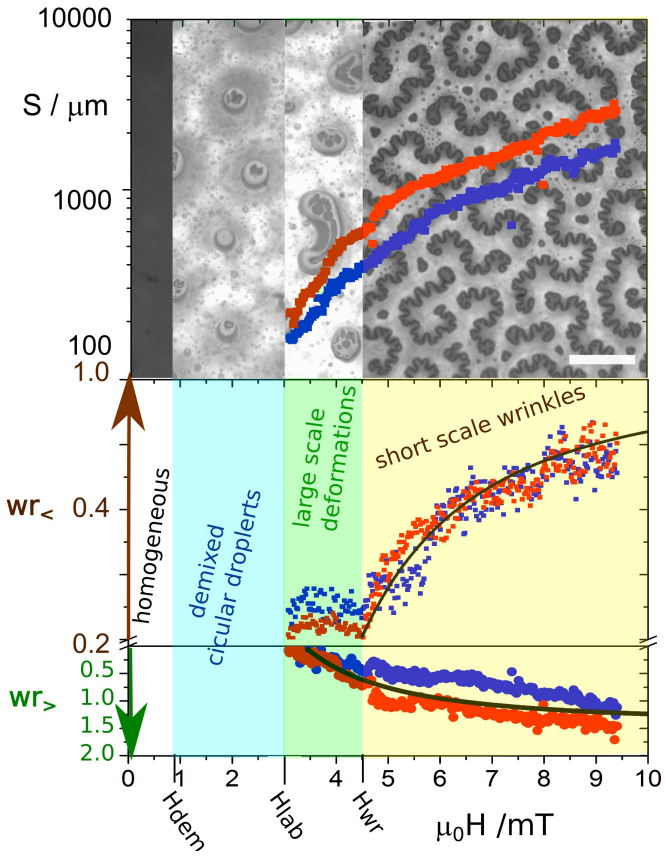

Fig. 5 Plot of the surface path length S, the small scale wrinkle number $wr_<$, and the large scale wrinkle number $wr_>$ versus the external magnetic field for the structures marked with red and blue in fig. 1. Small scale wrinkles only occur after the circle versus dogbone/labyrinth transition. The black lines are fits according to equation 5 and a similar equation for $wr_>$. Scale bar in the images is $100\,\mu$m. A movie of the sequence of transitions can be viewed in [35].

face path length soon catches up with the bulk due to its smaller Bond number. When the surface length becomes larger than the bulk this is the situation when the surface path has to start wrinkling. This explains why the wrinkling transition happens after the circle-to-dog-bone (labyrinth) transition.

Inserting equation 4 into equation 2 we obtain a theoretical prediction for the small scale wrinkles:

$$wr_< = \ln\left(\frac{A_s\xi_b}{A_b\xi_s}\right) + \frac{1}{2}\left(\frac{1}{N^b_{Bo}} - \frac{1}{N^s_{Bo}}\right) \qquad (5)$$

The black lines in figure 5 are fits ($A_s\xi_b/A_b\xi_s = 30$, $H^2/2(1/N^b_{Bo} - 1/N^s_{Bo}) = 13\ (\mathrm{mT})^2$) to the measured wrinkle numbers using equation 5 for $wr_<$, a similar equation for $wr_>$, and the assumption that the air/liquid interface moves the interfacial liquid away from the critical demixing point. In the case

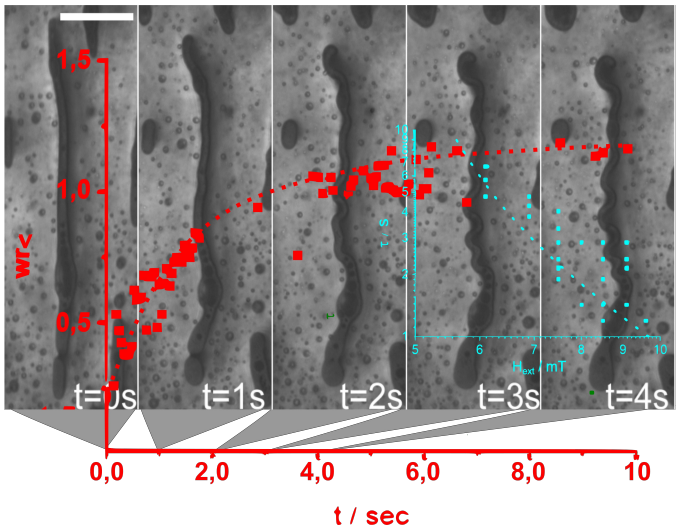

Fig. 6 Relaxation of an unwrinkled extended droplet back to its wrinkled equilibrium shape after switching of an oscillating in plane field for a normal field of $6.3\,\mathrm{mT}$. The scale bar is $50\,\mu\mathrm{m}$. We extract a plot of the small scale wrinkle number $wr_<(t)$ as a function of time (red) from the images of such movie for a normal field of $6.9\,\mathrm{mT}$. The relaxation time τ extracted from such graph is plotted versus the normal external field in the inset (cyan). It follows a $\tau \propto 1/H_{ext}(H_{ext} - H_{wr})$ behavior that is expected theoretically when assuming magnetic forces to be balanced by viscous forces. A movie of the relaxation can be viewed in [35].

that the interface moves the liquid closer to the critical demixing point the interfacial path length will not grow longer than the bulk path length and because we assume that the bulk enslaves the surface, the bulk will not be wrinkled by the surface. This is what we believe happens in our experimental mixture in figure 3 when covering the liquid with a glass cover slip.

The wrinkles are a thermodynamic equilibrium structure that does not depend on transport coefficients such as the viscosity. We can erase the wrinkles using an in plane oscillating magnetic field of strength 1.6 mT and frequency 10 Hz superposed to the static normal field. An in-plane field in the y-direction induces smooth stripe patterns that relax back to a wrinkled labyrinth when we switch off the in-plane field. In Fig. 6 we depict the pattern for various times after switching off the in-plane field. One can clearly see the relaxation into a wrinkled structure (see the movie Relaxation.avi in the supporting information [35]). In Fig. 6 we plot the time dependence of the small scale wrinkle number $wr_<(t)$ versus the time (red). The experimental relaxation can be described by a sigmoidal relaxation process:

$$wr_<(t) = wr^\infty_< \tanh((t - t_0)/\tau) \qquad (6)$$

with a relaxation time $\tau(H_{ext}) \propto 1/H_{ext}(H_{ext} - H_{wr})$ (blue). Such relaxation time dependence is expected from the balance of magnetic (that depend on the product of the magnetic field and

View Article Online
DOI: 10.1039/C7SM01475A

the magnetization, and must vanish for $H_{ext} - H_{wr}$) and viscous forces (that do not depend on the magnetic field).

In conclusion, a ferrofluid mixture close to a critical demixing point is sensitive enough to have substantially different properties near a surface as compared to the bulk. The differences in properties result in different equilibrium lengths of the surface and bulk path lengths of droplets having undergone a dipolar shape transition. Since both parts of the droplets are coupled, the longer surface path has to wrinkle. The experimental geometry of the wrinkles agrees well with predictions taken of both path lengths from well known theories about modulated phases.

1 Acknowledgement

NW thanks the Alexander von Humboldt foundation for a AvH fellowship. J. B acknowledges financial support by a Ghana MOE - DAAD joined fellowship. We thank Florian Johannes Maier for helping with the numerical analysis of the droplets.

References

1 E. Cerda, and L. Mahadevan; Geometry and physics of wrinkling *Phys. Rev. Lett.* **90**, 074302, (2003).

2 N. Liu, Z. Pan, L. Fu, C. Zhang, B. Dai, Z. and Liu; The origin of wrinkles on transferred graphene, *Nano Research* **4**, 996-1004, (2011).

3 J. Huang, M. Juszkiewicz, W. H. de Jeu, E. Cerda, T. Emrick, N. Menon, T. P. Russell; Capillary wrinkling of floating thin polymer films *Science* **317**, 650-653 (2007).

4 K. Efimenko, M. Rackaitis, E. Manias, A. Vaziri, L. Mahadevan, and J. Genzer; Nested self-similar wrinkling patterns in skins *Nature materials* **4**, 293-297, (2005).

5 M. Seul, and D. Andelman; Domain Shapes and Patterns: The Phenomenology of Modulated Phases *Science* **267**, 476-483 (1995).

6 H. Wang, Y. Zhu, C. Boyd, W. Luo, A. Cebers, and R. E. Rosensweig; Periodic branched structures in a phase-separated magnetic colloid *Phys. Rev. Lett.* **72**, 1929-1932 (1994).

7 Yu A. Buyevich and A. O. Ivanov; Equilibrium properties of ferrocolloids, *Physica* A **190**, 276-294 (1992).

8 A. Yu Zuberev, and L. Yu Iskakova; Condensation phase transitions in ferrofluids, *Physica* A **335**, 325-338 (2004).

9 A. Yu. Zubarev and L. Yu. Iskakova; Direct and inverse domain structures in ferrofluids, *Physica* A **367**, 55-68 (2006).

10 A. Yu. Zubarev and L. Yu. Iskakova, Yield stress in thin layers of ferrofluids, *Physica* A **365**, 265-281 (2006).

11 L. Yu. Iskakova, A. P. Romanchuk, and A. Yu. Zuberev, Phase and structural transformations in magnetorheological suspensions, *Physica* A **366**, 18-30 (2006).

12 V. S. Mendelev and A. O. Ivanov; Ferrofluid aggregation in chains under the infuence of a magnetic field, *Physical Review E* **70**, 051502 (2004).

13 Yu. A. Buyevich and A. Yu. Zubarev; Domain structures in thin layers of a ferrocolloid, *J. Phys. II France* **3**, 1633-1645 (1993).

14 A. G. Papathanasiou, and A. G. Boudouvis; Three-lobe-shaped equilibrium states in magnetic liquid bridges, *Phys. Rev. E* **65**, 035302 (2002).

15 R. E. Rosensweig, M. Zahn, and R. Shumovich, Labyrinthine instability in magnetic and dielectric fluids, *J. Magn. Magn. Mater.* **39**, 127-132 (1983).

16 J. E. Martin and J. Odinek; Evolution of structure in a quiescent Electrorheological fluid, *Phys. Rev. Lett.*, **69**, 1524-1527 (1992).

17 H. McConnell; Structures and Transitions in Lipid Monolayers at the Air-Water Interface *Annual Review of Physical Chemistry* **42**, 171-195 (1991).

18 K. Y. C. Lee, H. M. McConnell; Quantized symmetry of liquid monolayer domains *J. Phys. Chem.* **97**, 9532-9539 (1993).

19 H. A. Stone and H. M. McConnell; Hydrodynamics of Quantized Shape Transitions of Lipid Domains *Proceedings: Mathematical and Physical Sciences* **448**, 97-111 (1995).

20 P. Heinig, P. Steffen, S. Wurlitzer, and T. M. Fischer; Two-Dimensional Pendant Droplet Tensiometry in a Langmuir Monolayer *Langmuir* **17**, 6633-6637 (2001).

21 A. H. Eschenfelder; Magnetic bubble technology (Springer Verlag, Berlin, 1980).

22 C. L. Dennis,R. P. Borges, L. D. Buda, U. Ebels, J. F. Gregg, M. Hehn, E. Jouguelet, K. Ounadjela, I. Petej, I. L. Prejbeanu, and M. J. Thornton; The defining length scales of mesomagnetism: a review, *J. Phys.: Condens. Matter* **14**, R1175-R1262 (2002).

23 H. Vandeparre, M. Piñeirua, F. Brau, B. Roman, J. Bico, C. Gay, W. Bao, C. N. Lau, P. M. Reis, and P. Damman; Wrinkling Hierarchy in Constrained Thin Sheets from Suspended Graphene to Curtains *Phys. Rev. Lett.* **106**, 224301, (2011).

24 M. He, N. Xin, Y. Liu and Y. Zhang; Determination of critical properties for binary and ternary mixtures of short chain alcohols and alkanes using a flow apparatus, *The Journal of Supercritcal Fluids*, **104**, 19-28 (2015).

25 C. A. Grattoni, R. A. Dawe, C. Y. Seah, and J. D. Gray; Lower Critical Solution Coexistence Curve and Physical Properties (Density, Viscosity, Surface Tension, and Interfacial Tension) of 2,6-Lutidine + Water, *J. Chem. Eng. Data*, **38**, 516-519 (1993).

26 I. Szalai and S. Dietrich; Global phase diagrams of binary dipolar fluid mixtures, *Molecular Physics* **103**, 2873 - 2895 (2005).

27 S. M. Cattes, S. H. L. Klapp; and Martin Schoen, Condensa-

View Article Online
DOI: 10.1039/C7SM01475A

tion, demixing, and orientational ordering of magnetic colloidal suspensions, *Physical Review* E **91**, 052127 (2015).

28 K. Lichtner, A. J. Archer, and S. H. L. Klapp; Phase separation dynamics in a two dimensional magnetic mixture, *Journal of Chemical Physics* **136**, 024502 (2012).

29 B. Groh and S. Dietrich; Ferroelectric phase in Stockmayer fluids *Phys. Rev. E.* **50**, 3814-3833 (1994).

30 B. Groh and S. Dietrich; Long-ranged orientational order in dipolar fluids *Phys. Rev. Lett.* **72**, 2422-2425 (1994).

31 A. B. Yener and S. H. L. Klapp; Self-assembly of three-dimensional ensembles of magnetic particles with laterally shifted dipoles, *Soft matter* **12**, 2066-2075 (2016).

32 J. Bugase, J. Berner, and Th. M. Fischer; Magnetic field induced modulated phases in a ferrofluid lutidine silicone oil mixture *Soft Matter*, **12**, 8521-8527 (2016).

33 Note that the phase depleted of ferrofluid is fully transparent, and we can resolve objects also in the bulk of the fluid mixture.

34 The images are binarized, skeletonized, and dangling branches are cut off the skeleton to produce a curve $\mathbf{r}(s)$. The distance $s - s$ is then computed from the distances of consecutive pixels. Since the skeletonized curve has a thickness of one pixel there is some chance that the skeletonization of the curve will cut a single real droplet into virtual two droplets. This is what happens in the top of figure 5 at some data points near $H = 7$ mT and $H = 8$ mT. One droplet is wrongly split into two by the skeletonization. The wrinkle number does not react to the splitting.

35 A movie *Transitions.avi* showing the sequence of transitions and a movie *Relaxation.avi* showing the relaxation from stretched droplets versus the wrinkled state is available free of charge under XXXXXXXXX

36 R. de Koker, H. M. McConnell; Circle to dogbone: shapes and shape transitions of lipid monolayer domains *J. Phys. Chem.* **97**, 13419-13424 (1993).

37 D. Andelman and R. E. Rosensweig; "The Phenomenology of Modulated Phases: From Magnetic Solids and Fluids to Organic Films and Polymers" in "Polymers, Liquids and Colloids in Electric Fields: Interfacial Instabilities, Orientation, and Phase-Transitions", Ed. by Y. Tsori and U. Steiner, Vol. 2 in "Series in Soft Condensed Matter", (World Scientific, Singapore, 2009), chapter 1, pp. 1-56.

View Article Online
DOI: 10.1039/C7SM01475A